arXiv:1212.0832v1 [quant-ph] 4 Dec 2012

Experimental implementation of assisted quantum adiabatic passage in a single spin

Jingfu Zhang[1], Jeong Hyun Shim[1], Ingo Niemeyer[1], T. Taniguchi[2], T. Teraji[2],
H. Abe[3], S. Onoda[3], T. Yamamoto[3], T. Ohshima[3], J. Isoya[4] and Dieter Suter[1]
[1]Fakultät Physik, Technische Universität Dortmund, D-44221 Dortmund, Germany
[2]National Institute for Materials Science, 1-1 Namiki, Tsukuba, Ibaraki, 305-0044 Japan
[3]Japan Atomic Energy Agency, 1233 Watanuki, Takasaki, Gunma, 370-1292 Japan
[4]Research Center for Knowledge Communities, University of Tsukuba, Tsukuba, 305-8550 Japan
(Dated: December 5, 2012)

Quantum adiabatic passages can be greatly accelerated by a suitable control field, called a counter-diabatic field, which varies during the scan through resonance. Here, we implement this technique on the electron spin of a single nitrogen-vacancy center in diamond. We demonstrate two versions of this scheme. The first follows closely the procedure originally proposed by Demirplak and Rice (J. Phys. Chem. A 107, 9937 (2003)). In the second scheme, we use a control field whose amplitude is constant, but its phase varies with time. This version, which we call the rapid-scan approach, allows an even faster passage through resonance and therefore makes it applicable also for systems with shorter decoherence times.

PACS numbers: 03.67, 33.35, 76.70

Introduction.– Controlling quantum systems with high fidelity is an essential prerequisite in various fields, such as coherent control of atomic and molecular systems [1] and quantum information processing [2, 3]. The strategies that have been developed for this purpose include the adiabatic passage technique, which leads the quantum system along a specific pathway in such a way that the system always remains in its ground state. One of the attractive properties of this technique is that the resulting evolution is robust with respect to some experimental imperfections [4]. Adiabatic passage also is the central part of the adiabatic model of quantum computation [5, 6], which has been shown to be equivalent to the more common network model. In all these cases, it is essential that the scan duration of the adiabatic passage is short and the fidelity as high as possible.

The quantum adiabatic theorem guarantees that the system remains approximately in its ground state if the evolution is sufficiently slow [7–9]. However, for all practical applications, the optimal implementation is reached when the scan time remains short, e.g. compared to the decoherence time. This conflict can be relieved by an additional control field, the so-called the counter-diabatic (CD) field [10]. This strategy was recently implemented in an atomic Bose-Einstein condensate [11].

In this Letter, we report another experimental implementation of the assisted adiabatic passage (AAP), using a single nitrogen vacancy (NV)-center in diamond. The NV-center system is one of the promising candidate quantum bits (qubits) for building quantum computers [12, 13]. Various techniques for implementing high-fidelity coherent control of the NV-centers have been developed recently [14–16]. In our experiment, we implement the AAP on an electron spin transition of the NV-center, using resonant microwave fields as controls. The fidelity of the passage is sufficiently high that we can perform multiple rounds of the passage in opposite directions. The results show good agreement between theory and experiment. In contrast to the previous implementation where the coherent control was applied to an ensemble of atoms[11], our experiment is implemented on a single spin in one NV-center.

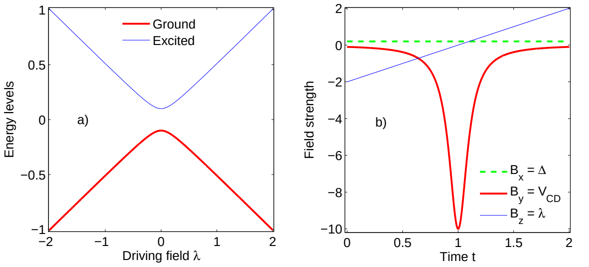

FIG. 1: (color online). Characteristics of the single qubit model for $\Delta = 0.2$ and $b = 2$. (a) shows the energy levels and (b) the time dependence of the three field components.

Model.– In close analogy to the Landau-Zener model [17–19], we describe the AAP with the Hamiltonian

$$H_{LZ}(t) = \lambda(t) I_z + \Delta I_x, \qquad (1)$$

where the $I_{x,z}$ are spin operators, and $\lambda(t)$ and Δ are dimensionless fields applied along the z and x directions. This Hamiltonian is a model for an arbitrary two level system and plays a prominent role in various fields of physics, such as in coherent control [11, 20] and quantum criticality [21–23]. The energy eigenvalues are $\pm\sqrt{\lambda^2(t) + \Delta^2}/2$, and the instantaneous ground state is

$$|g(t)\rangle = \sin\frac{\theta(t)}{2}|0\rangle - \cos\frac{\theta(t)}{2}|1\rangle, \qquad (2)$$

where $\tan\theta(t) = \Delta/\lambda$, $\theta \in [0, \pi]$, and $|0\rangle$ and $|1\rangle$ denote the eigenstates of I_z with eigenvalues $\pm 1/2$, respectively. The minimal gap between the two levels is Δ. Fig. 1 (a) illustrates the energy levels for $\Delta = 0.2$. For the initial

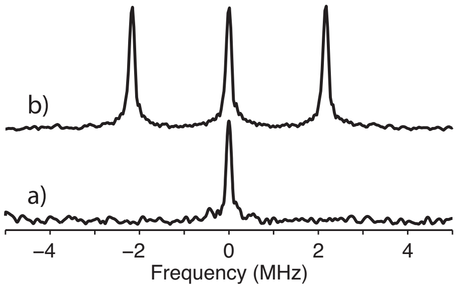

FIG. 2: Spectra of the NV electron spin obtained by a) transition selective and b) hard pulses.

discussion, we assume that the control field is scanned linearly with time,

$$\lambda(t) = b(t-1), \tag{3}$$

where $t \in [0, 2]$, and b represents the scan range of λ, which is $[-b, b]$, and also its rate of change.

The assisted adiabatic passage can be implemented for any non-zero value of Δ by introducing a CD field that is perpendicular to both the x-component Δ and the z-component $\lambda(t)$ of the field: [10, 23]

$$H_{CD}(t) = V_{CD}(t) I_y \tag{4}$$

where

$$V_{CD}(t) = -\frac{b\Delta}{[\Delta^2 + \lambda(t)^2]}. \tag{5}$$

The total field for the AAP is thus a vector $\vec{B}(t) = [\Delta, V_{CD}(t), \lambda(t)]$. Fig. 1 (b) shows the time dependence of the three components for $b = 2$.

Experimental protocols and results.– For the experimental test, we used the electron spin of a single NV-center in ^{12}C enriched diamond. The sample used is a diamond single crystal grown at 5.5 GPa and 1400 °C from Co-Ti-Cu alloy by using a temperature gradient method. As a solid carbon source we used polycrystalline diamond plates synthesized by chemical vapor deposition (CVD) utilizing ^{12}C enriched methane. According to the secondary ion mass spectroscopy analysis, ^{12}C enrichment of 99.995% was achieved in the grown crystals. The crystal was irradiated by 2 MeV electrons with a total fluence of 10^{11} e/cm^2 at room temperature and subsequently annealed at 1000 °C for 2 hours in vacuum. The reduced number of ^{13}C nuclear spins results in long relaxation times, with $T_2^* > 100\,\mu$s.

As shown in Fig. 2, the hyperfine coupling between the electron and the ^{14}N nuclear spin is ≈ 2.1 MHz. For the present experiments, we use the subspace of this system that is spanned by the states $m_S = 0, +1$ of the electron spin, $m_I = 0$ of the nuclear spin. As shown in Fig. 2 a), this subsystem can be excited with excellent selectivity if the amplitude of the microwave field remains well below the hyperfine coupling constant. We therefore will not consider the nuclear spin state in the following.

For the AAP, the system should be initialized into the ground state $|g(0)\rangle$ of $H_{LZ}(0)$. In the experiment, we initialize the system by a laser pulse into the state $|0\rangle$, whose overlap with $|g(0)\rangle$ is $\sin[\theta(0)/2]$. In the experiment, we use $-3 \geq \lambda(0)/\Delta \geq -20$, which results in overlaps of $[0.9871, 0.9997]$. For our purpose, this is sufficiently close to unity.

After initialization, the system evolves under the time-dependent Hamiltonian

$$H(t) = H_{LZ}(t) + H_{CD}(t) \tag{6}$$

into the state

$$|\psi(t)\rangle = \widetilde{U}(t)|g(0)\rangle, \tag{7}$$

where $\widetilde{U}(t)$ represents the propagator generated by $H(t)$. During and after the scan, we read out the state of the system by a second laser pulse, which again projects the system onto the state $|0\rangle$. We write the probability of finding the system in this state as $P_{|0\rangle} = |\langle 0|\psi(t)\rangle|^2$.

In the actual experiment, the fields Δ, V_{CD} and λ act on the spin in a rotating reference frame. Writing

$$U_r = e^{-i\xi(t) I_z}$$

for the transformation from the laboratory-frame to the rotating frame, the Hamiltonians of the two frames are related as

$$\begin{aligned} H^{\text{rot}} &= U_r H^{\text{lab}} U_r^\dagger + i\dot{U}_r U_r^\dagger \\ H^{\text{lab}} &= U_r^\dagger H^{\text{rot}} U_r - i U_r^\dagger \dot{U}_r. \end{aligned} \tag{8}$$

The laboratory-frame Hamiltonian thus has the field components

$$\begin{aligned} \omega_x(t) &= \Delta \cos\xi(t) + V_{CD}(t)\sin\xi(t) \\ \omega_y(t) &= -\Delta \sin\xi(t) + V_{CD}(t)\cos\xi(t) \\ \omega_z &= \lambda(t) - \frac{d\xi(t)}{dt}. \end{aligned}$$

This Hamiltonian must match the experimentally available Hamiltonian, whose general form is

$$H^{\text{exp}} = -\omega_0 I_z + 2\omega_1(t) I_x.$$

Accordingly, we must have

$$\xi(t) = \omega_0 t + \int_0^t \lambda(t')dt',$$

which defines our rotating frame transformation. For the transverse field components, we invoke the rotating field approximation, which allows us to set

$$\omega_1(t) = \Delta \cos\xi(t) + V_{CD}(t)\sin\xi(t)$$

and ignore the y-component. The amplitude of the field is therefore

$$|\omega_1(t)| = \sqrt{\Delta^2 + V_{CD}(t)^2}.$$

Experimental limitations define a maximum possible field amplitude, which we designate as Ω. In the present experiment, it is determined by the requirement that no transitions of other nuclear spin states are excited, and we found a value of $\Omega \approx 2\pi \cdot 0.2\,\mathrm{MHz}$ to be a suitable compromise. The maximum field amplitude is reached at

$$\Omega = \frac{\sqrt{\Delta^2 + \frac{b^2}{\Delta^2}}}{s_a}, \tag{9}$$

where we have defined the scale factor s_a, which converts the dimensionless quantities Δ and b into actual field amplitudes (in Hz) and defines the scan duration

$$\tau_s = 2 s_a. \tag{10}$$

Figure 3 shows the experimental results of the AAP for the scan rates $b = 0.6$, 1, 1.6, 2, 3 and 4. For these parameters, we can approximate $s_a \approx b/(\Omega\Delta)$. For $b = 0.6$, the scan duration becomes $4.77\,\mu$s and for $b = 4$ it is $31.83\,\mu$s. The z-component is always scanned from -40 to $+40$ kHz (in frequency units), while the y-component (the CD field) reaches a maximal amplitude of 200 kHz at the anticrossing point. The x-component of the field in the rotating frame is 13.3 kHz for $b = 0.6$ and 2.0 kHz for $b = 4$. Filled circles show the experimentally measured overlaps of the state with the ground state $|0\rangle$. The error bars (1 standard deviation) were determined by repeating each experiment 10 times. The solid lines, which agree very well with the experimental data points, represent the theoretical behavior. For comparison, we also show one data set that was obtained without CD field, for a scan rate of $b = 2$. These data points are represented by the empty circles and the corresponding theoretical curve can be approximated as a horizontal line going through the experimental points. Clearly, a passage without CD field results in an almost completely diabatic transfer.

A significant additional speedup over this direct implementation of the AAP scheme is possible if the amplitude of the control field is kept constant throughout the scan, at the maximum value that is experimentally accessible. For this purpose, we divided the total evolution period into N segments with identical duration δ [24, 25]. The propagator $\widetilde{U}(t)$ generated by $H(t)$ can then be implemented by a series of discrete unitary operators U_m for each period:

$$\widetilde{U}(j\delta) \approx \prod_{m=1}^{j} U_m. \tag{11}$$

For each segment, the propagator $U_m = e^{-i\delta H(m\delta)}$ was implemented as a rectangular pulse with the amplitude Ω, which is the same for all segments. With this approach, we expect to increase the possible scan rate. The total number N of these segments must be large enough that this discrete version becomes a good approximation of the continuous scan.

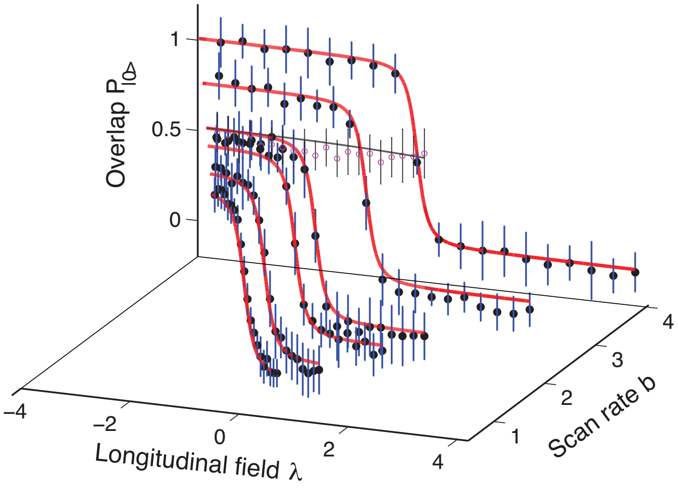

FIG. 3: (color online). Experimental results obtained with the analog implementation of the AAP. The individual experiments correspond to $b = 0.6$, 1, 1.6, 2, 3 and 4. The experimental data are shown as filled circles, and the corresponding error bars were obtained by repeating the experiment 10 times. The curves show the theoretical result for an ideal scan. The empty circles with the almost horizontal line show the result for a reference experiment without CD field.

We calculate the Hamiltonians H_m for the individual segments from the requirement that

$$U_m = e^{-i\delta H(m\delta)} = e^{-i\tau_m H_m},$$

where τ_m is the duration of the pulse that implements the m^{th} segment and H_m the experimentally realized Hamiltonian in the rotating frame. We can therefore reduce the duration of this segment by a factor $s_m = \tau_m/\delta$ if we simultaneously scale up the Hamiltonian, $H_m = H(m\delta)/s_m$. Using the transformation (8), we can calculate the required laboratory-frame Hamiltonian

$$H_m^{\mathrm{lab}} = -\omega_0 I_z + 2\Omega I_x \cos(\omega_m t + \phi_m)$$

and the required duration τ_m. The scaling factor

$$s_m = \frac{\tau_m}{\delta} = \frac{\sqrt{\Delta^2 + V_{CD}^2(m\delta)}}{\Omega} \tag{12}$$

is now different for every segment. The angular frequency ω_m and the phase ϕ_m become

$$\omega_m = \omega_0 + \frac{\lambda(m\delta)}{s_m}, \qquad \tan\phi_m = -\frac{V_{CD}(m\delta)}{\Delta}.$$

Figure 4 shows the experimental results. Here, we used the same nominal scan rates b as in the analog case, but split the scan into $N = 56$ segments. The experimental data points are represented by filled circles, the error bars were obtained by repeating the experiments 8 times. Clearly, the experimental data agree very well with the theoretical expectation shown as the red curves. The

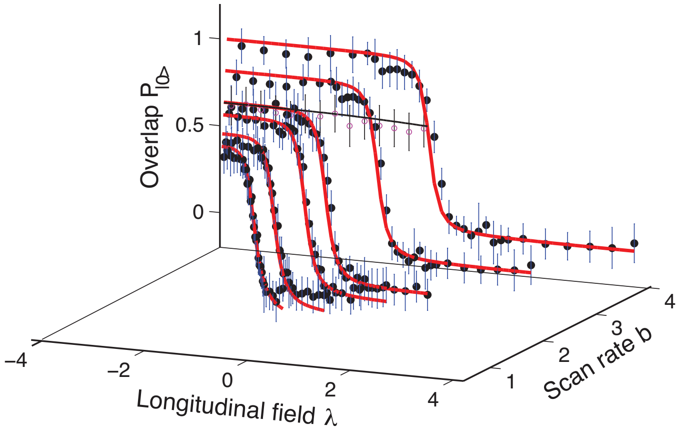

FIG. 4: (color online). Experimental results obtained with the rapid-scan approach. For details see the caption of Fig. 3.

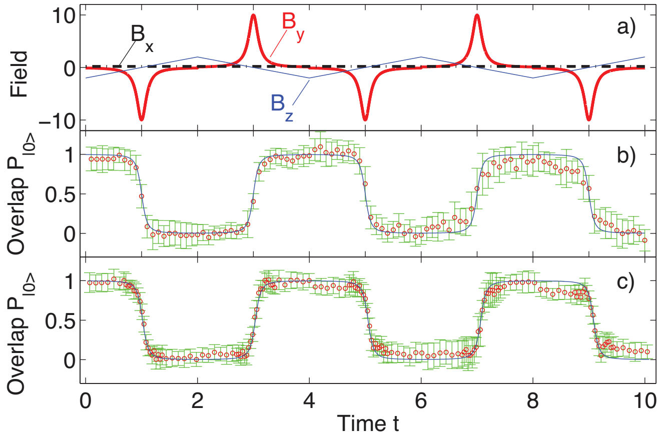

FIG. 5: (color online). Multiple assisted adiabatic passages. (a) shows the time-dependence of the three field components, while b) and c) show the experimental data, together with the theoretical curves for the ideal case (zero loss).

empty circles again represent the reference experiment obtained by setting $V_{CD} = 0$.

Given the high fidelity obtained in a single passage through resonance, we can cycle the system forth and back multiple times. The reverse passage is obtained by changing b to $-b$, which changes the direction of the scan as well as the sign of the CD field. Figure 5 a) shows the time-dependence of all three field components in the rotating frame. Figures 5 b) and c) represent the experimental results for these repetitive scans, as well as the theoretical curves corresponding to the ideal case. We find very little loss of population after five passages through resonance.

Discussion.– The experimental implementation of the time-dependent Hamiltonian $H(t)$ always occurs with finite precision, which results in a loss of fidelity. Experimental contributions to this loss include the precision with which the shaped pulses are implemented - both in terms of the amplitude as well as in terms of the time resolution. In the rapid-scan approach, the number of segments used is an important parameter. We used numerical simulations of the experiment to estimate these losses. The results indicate that for the analog scan, finite time resolution of 0.25 ns reduces the fidelity by a fraction of the order of 10^{-8}. In the rapid-scan approach, for $N = 56$ segments, the maximal loss during the AAP occurs near the critical point at $\lambda = 0$. For the lowest scan rate, with $b = 0.6$, this loss is of the order of $< 10^{-3}$, for the faster scan rate, $b = 4.0$, it rises to $2.8 \cdot 10^{-2}$. However, these are mostly intermediate losses, which are recovered during the second part of the scan: The calculated loss of fidelity at the end of the evolution period is $< 10^{-4}$.

For the parameters chosen here, the duration of a single scan varies between 4.77 and 31.83 μs in the analog version and from 2.0 to 2.5 μs in the rapid scan implementations. They are thus all short compared to the coherence time of our sample ($T_2 \approx 500 \mu s$).

To estimate the speed-up provided by the CD field, we used numerical simulations of an unassisted scan, with the same parameters as the experimental scan in Fig. 3, but slower scan rates. To reach a fidelity of 0.99, the scan duration had to be extended to 2.33 ms. This implies that the assisted scan allows a speedup of more than two orders of magnitude (~ 150) if a linear frequency scan is used and of about three orders of magnitude (~ 960) in the rapid passage (constant amplitude) version.

Conclusion.– We have implemented the assisted adiabatic passages through analog and rapid-scan approaches in a two level quantum system by controlling a single spin in a NV-center in diamond. This approach allows a significant increase in the scan rate compared to the unassisted passage and therefore reduces the requirements on the decoherence time of the system to which it is applied. Like in the unassisted case, the scan has to be slower if the minimum gap is small. If the scan is performed linearly in time, the total duration also increases with the scan range. However, with the rapid-scan approach that we introduced here, the scan range can be increased arbitrarily with very little time-penalty. Our experiment results illustrate the excellent coherent control that can be achieved for the spins of NV-centers. These results should be helpful for all applications requiring quantum adiabatic passages, such as implementing geometric gates for quantum computation [26], adiabatic control in interacting two level systems [27] or adiabatic quantum computing [6].

This work is supported by the Heinrich Hertz Foundation, and the DFG through grant Su 192/27-1.

---

[1] P. Král, I. Thanopulos and M. Shapiro, Rev. Mod. Phys. **79**, 53 (2007).

[2] M. Nielsen and I. Chuang, *Quantum Computation and Quantum Information* (Cambridge University Press, Cambridge, 2000).

[3] J. Stolze and D. Suter, *Quantum Computing: A Short Course from Theory to Experiment* (Wiley-VCH, Berlin, 2nd edition, 2008).

[4] A. M. Childs, E. Farhi and J. Preskill, Phys. Rev. A **65**, 012322 (2001).

[5] E. Farhi, J. Goldstone, S. Gutmann and M. Sipser, arXiv:quant-ph/0001106v1 (2000).

[6] E. Farhi, J. Goldstone, S. Gutmann, J. Lapan, A. Lundgren and D. Preda, Science, **292**, 472 (2001).

[7] J. Du, L. Hu, Y. Wang, J. Wu, M. Zhao and D. Suter, Phys. Rev. Lett. **101**, 060403 (2008).

[8] D. M. Tong, K. Singh, and L. C. Kwek and C. H. Oh, Phys. Rev. Lett. **95**, 110407 (2005).

[9] K.-P. Marzlin and B. C. Sanders, Phys. Rev. Lett. **93**, 160408 (2004).

[10] M. Demirplak and S. A. Rice, J. Phys. Chem. A **107**, 9937 (2003).

[11] M. G. Bason, M. Viteau, N. Malossi, P. Huillery, E. Arimondo, D. Ciampini, R. Fazio, V. Giovannetti, R. Mannella and O. Morsch, Nature Physics, **8**, 147 (2012).

[12] T. D. Ladd, F. Jelezko, R. Laflamme, Y. Nakamura, C. Monroe and J. L. O'Brien, Nature, 464, 45 (2010).

[13] D. DiVincenzo, Nature Materials, **9**, 468 (2010).

[14] J. Wrachtrup and F. Jelezko, J. Phys.: Condens. Matter, **18**, S807 (2006).

[15] T. van der Sar, Z. H. Wang, M. S. Blok, H. Bernien, T. H. Taminiau, D. M. Toyli, D. A. Lidar, D. D. Awschalom, R. Hanson and V. V. Dobrovitski, Nature, **484**, 82 (2012).

[16] X. Xu et al., Phys. Rev. Lett. **109**, 070502 (2012).

[17] L. D. Landau and E. M. Lifshitz, *Quantum Mechanics* (Pergamon, London, 1958).

[18] C. Zener, Proc. R. Soc. London **A**, **137**, 696 (1932).

[19] S. N. Shevchenko, S. Ashhab and F. Nori, Phys. Rep. **492**, 1 (2010).

[20] E. Barnes and S. D. Sarma, Phys. Rev. Lett. **109**, 060401 (2012).

[21] B. Damski, Phys. Rev. Lett. **95**, 035701 (2005).

[22] F. M. Cucchietti, J.-F. Zhang, F. C. Lombardo, P. I. Villar and R. Laflamme, Phys. Rev. Lett. **105**, 240406 (2010).

[23] A. del Campo, M. M. Rams and W. H. Zurek, Phys. Rev. Lett. **109**, 115703 (2012).

[24] R. Somma, G. Ortiz, J. E. Gubernatis, E. Knill and R. Laflamme, Phys. Rev. A **65**, 042323 (2002).

[25] X. Peng, J. Du and D. Suter, Phys. Rev. A **71**, 012307 (2005).

[26] H. Wu et al., arXiv:1208.0555 [quant-ph] (2012).

[27] R. T. Brierley, C. Creatore, P. B. Littlewood and P. R. Eastham, Phys. Rev. Lett. **109**, 043002 (2012).